Optical temperature sensor and thermal expansion measurement using a femtosecond micro-machined grating in 6H-SiC

G. Logan DesAutels[1], Peter Powers[3], Chris Brewer[2], Mark Walker[4], Mark Burky[1], Gregg Anderson[2]

[1]AT&T Government Solutions, Dayton, OH 45433
[2]Air Force Research Laboratory, Materials and Manufacturing Directorate, WPAFB, OH 45433
[3]University of Dayton, Dayton, OH 45469
[4]General Dynamics Information Tech., Dayton, OH 45431

Abstract – An optical temperature sensor was developed using a femtosecond micro-machined diffraction grating inside transparent bulk 6H-SiC. In addition to the temperature sensor, a measurement of the 6H-SiC thermal coefficient was made by means of the grating first order diffracted beam. A HeNe laser beam was used with the SiC grating to produce a first-order diffracted beam where the change in deflection height was measured as a function of temperature. The grating was micro-machined with a 20μm spacing and has dimensions of approximately 500μm x 500μm (l x w) and is roughly 0.5μm deep into the 6H-SiC bulk. A maximum temperature of 399°C was measured, which gives a ΔT of 372.3°C. The sensitivity of the technique is ΔT=5C? A maximum deflection angle of 1.81° was measured in the 1st order diffracted beam. The trend of the deflection with increasing temperature is a nonlinear polynomial of the 2nd order. This optical SiC thermal sensor has many high temperature electronic applications, such as, aircraft turbine and gas tank monitoring for commercial and military applications.

OCIS Codes: (280.6780), (050.7330).

1. Introduction

Diffraction gratings have a variety of applications, and are constructed by a number of techniques. The grating in this paper was fabricated using a femtosecond laser and an anamorphic lens[1], and then this grating was used in a new method of measuring temperature and the thermal coefficient of a sample. Bulk transparent 6H-SiC was selected to have a 500μm length x 500μm width x 0.5μm deep grating with 20μm spacing micro-machined using the anamorphic lens technique[1].

SiC is an attractive alternative material for a variety of semiconductor devices where silicon (Si) lacks the environmental resistance that carbon furnishes when combined to Si[2]. These areas where SiC devices can be used include high-power high-voltage switching applications, high temperature electronics, and avionics where it is desired to keep sensitive Si-based electronics and temperature sensors away from extreme environments onboard aircraft (such as turbines and fuel

compartments)[2]. For these reasons, it is of interest to study the use of SiC as a noncontact high temperature sensor. The SiC used for this study has the following characteristics shown in Table 1.

Table 1: SiC sample characteristics for semi-insulating type. The semi-insulating SiC sample used was supplied by Intrinsic Corp, and the gratings were micro-machined by the 1st author.

Sample	**Grating and Beam Orientation**	**Dopant**	**Dopant Concentration (cm^{-3})**	**Resistivity (Ω·cm)**	**Thickness (μm)**	**Face**
SiC semi-insulating	c-plane, 6H 0° on axis	Undoped	~$1x10^{15}$	$3x10^{7}$	340	Si

As a comparison, different types of temperature sensors were investigated as a comparison to the noncontact optical SiC sensor. As compared to other types of noncontact temperature sensors this method has a few advantages such as the measurement of temperature transparent/nontransparent materials, measurement of extremely high temperatures remotely, the ability to measure the coefficient of thermal expansion of transparent/nontransparent materials, and the ability to measure the coefficient of linear expansion of transparent/nontransparent materials.

2. Experimental Setup

Figure 1 gives the experimental setup for the SiC sensor data collect.

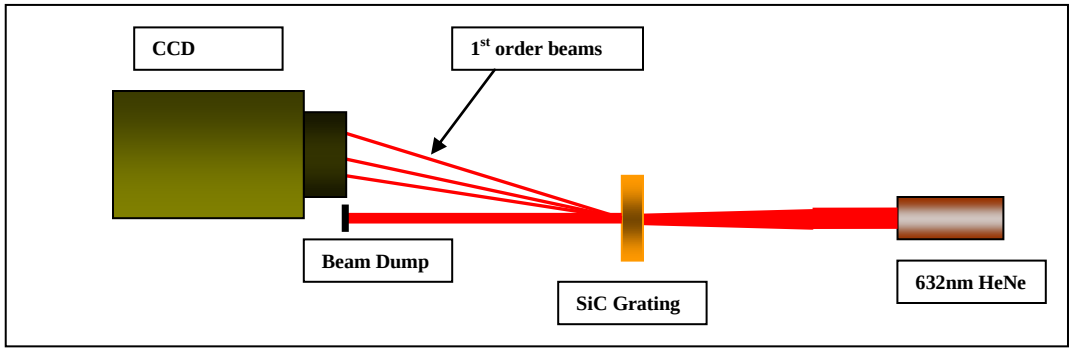

Figure 1 SiC temperature sensor experimental setup.

Figure 1 shows the setup for the SiC temperature sensor, which consists of a 632.8nm HeNe, the SiC grating seated in a copper mount, and a CCD camera to record the change in the 1st order height (Δx). The camera is a Cohu 4812 model and it utilizes Spiricon laser beam analysis software to measure the vertical centroid direction in microns. Each of the first order beams in the figure is representing different heights due to the increasing temperature (not to scale). The camera is calibrated against neutral density filters and the background lighting to a Fieldmax power meter. The total power from the 0-order to

the total power in the first order gives a measure of the grating efficiency; that was measured for completeness to be 0.6% ($DE = 2P_1/P_0$ – where the 2 represents the ±1 orders). The change in 1st-order beam height (Δx) was measured and plotted as a function of temperature.

The 6H-SiC grating was mounted in a 2.25" x 2.25" copper mount with a 0.5" square hole where the sample was placed so that the HeNe beam could propagate through the grating. The copper mount had two 1/8" diameters by 2" deep holes for the J-type thermal couple and the cartridge heater. The copper mount and SiC sample together were insulated with ceramic shielding and the SiC temperature was also monitored with a K-type thermal couple to ensure the grating was at the same temperature as the copper. The cartridge heater started at 26.7°C (about 10° above laboratory temperature) and in 50° increments was able to reach 399°C.

The temperature was measured and controlled with an Omega temperature controller CN7800 that has ±1° C resolution and with the ceramic insulation the measurements were consistently within ±3° C due to the temperature of the laboratory convection. Most of the error in measurement came from the Spiricon resolution, which has a spatial accuracy of ±0.5% and a beam width accuracy of ±2%. However, due to convection caused from the laboratory temperature, the 1st order deflected HeNe beam had a pointing stability of ~35%. This was observed at higher temperatures and is due to air convection from the cooler lab temperatures and the heated sample. Because of the thermal convection, the beam centroid was averaged for over 88,000 images (45 minutes time average for each data point) in order to drop the error in Δx measurement down to a maximum of ±1.2%. This measurement can be improved by imaging both the zero order and the 1st order spots so that the relative displacement can be measured. This would help to normalize out the effects of thermal convection. In addition, the 2nd or higher orders can be used to increase sensitivity.

3. Theoretical Results

The SiC temperature sensor is considered a volume transmission grating therefore standard diffraction grating theory was applied to predict the grating performance. The mechanism for the change in spacing of the grating is thermal expansion, which causes the grating spacing to expand thus results in the 1st order deflected beam to drop back to the 0-order. Initially it was assumed that the thermal coefficient of 6H-SiC would be linear, but it becomes nonlinear when the ΔT became too large for the linear approximation. Starting from the thermal coefficient and grating equations the change in grating spacing as a function of temperature, Δd, can be derived.

The 6H-SiC grating spacing, d, is initially 20μm and is changes by[3]

$$\Delta d = \alpha \cdot d \cdot \Delta T \qquad \text{Equation 1}$$

Where α is the coefficient of thermal expansion solved once Δd was found experimentally as shown in Figure 2. Equation 1 was applied to the grating equation as stated in Equation 2[4].

$$m\lambda = d \cdot (\sin(\theta) + \sin(\beta)) \qquad \text{Equation 2}$$

Here, in Equation 2, m is the order (m = 1), β is the input angle into the grating and θ is the reflection or transmit angle. The deflection (Δx) is derived by solving for θ in Equation 3 for the grating spacing and the change in the grating spacing as a function of temperature.

$$\Delta x = [\tan(\theta) \cdot L] - [\tan(\Delta\theta) \cdot L] \qquad \text{Equation 3}$$

Where L is the distance from the grating to the CCD camera and Δθ is given in Equation 4.

$$\Delta\theta = \sin^{-1}\left(\frac{\lambda}{(d + \Delta d)} - \sin(\beta)\right) \qquad \text{Equation 4}$$

From these equations the Δx can be predicted for each given temperature. Given the experimental Δx the thermal coefficient, α, can be calculated from backing out Δd and using Equation 1. The change in the grating spacing, Δd, is derived from the following equation.

$$\Delta d = \frac{\lambda - \tan^{-1}\left(\frac{x - \Delta x}{L}\right)}{\tan^{-1}\left(\frac{x - \Delta x}{L}\right)} \cdot d \qquad \text{Equation 5}$$

Where x is the original deflection before the temperature is increased. The experimental 2nd order polynomial thermal coefficient equation (α) can now be solved by relating the measured Δx values to derive Equation 5. Next, Δd, Equation 5, can be substituted into Equation 1 and plotted as a function of temperature in Figure 3, where a polynomial fit to the trend is applied that is shown in Equation 6 below.

$$\alpha = -1.38x10^{-11} \cdot \Delta T^2 + 1.23x10^{-8} \cdot \Delta T + 3.84x10^{-6} \qquad \text{Equation 6}$$

4. Experimental Results

The experimental results conclude that a maximum deflection for 399°C (starting from 26.7°C) was 140µm as shown in Figure 2 below.

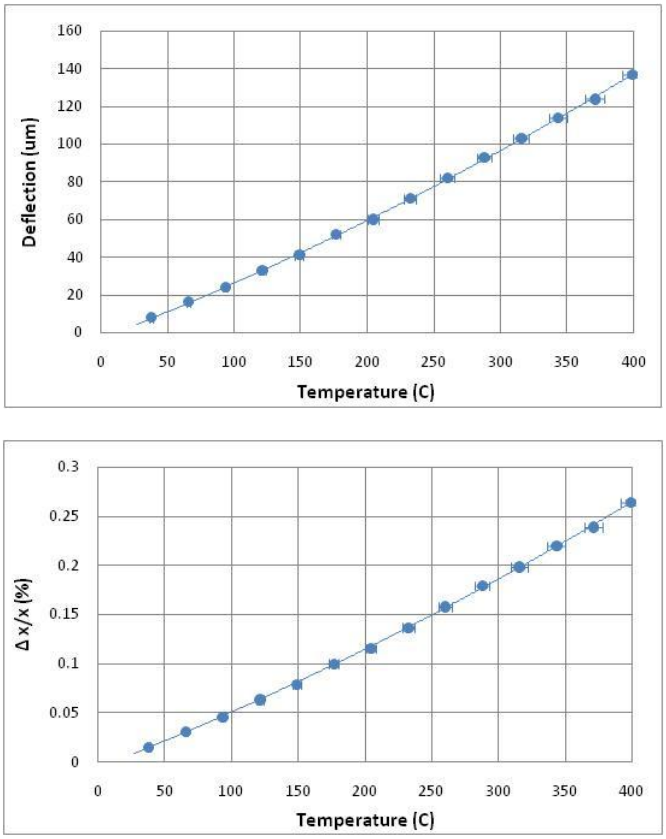

Figure 2 (Top) shows the deflection (Δx) as a function of temperature, (bottom) shows the Δx/x ratio as a function of temperature, which is a common way of displaying the material expansion. The charts show a max ~5% error bars.

The error bars for each data point is ±1.2% maximum as mentioned previously. The 1.2% error bars relate to 5°C absolute temperature variation. The maximum Δx for 1640mm from the grating is 140µm, which corresponds to 6.5×10^{-6} 1/°C from Equations 1, 2, 6, and shown in Figure 3. The percentage of the Δx/x for 400°C is 0.26%, which corresponds to the same findings of Bhatt *et al*[5].

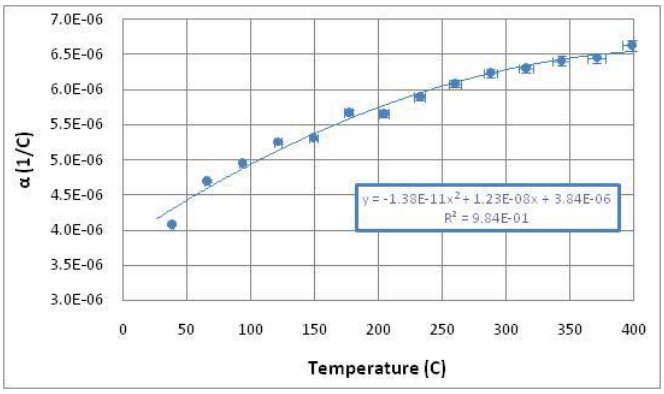

Figure 3 Shown here is the 6H-SiC thermal coefficient as a function of temperature with maximum 5% error bars. The 2nd order polynomial is given in Equation 1.

Figure 3 shows the nonlinear coefficient of thermal expansion as well as the coefficient of linear expansion (4.25×10^{-6} °C^{-1}) of 6H-SiC, which is in good agreement with Li *et al*, who also found the coefficient of thermal expansion to be a 2nd order polynomial trend for 4H-SiC[6] as well as a coefficient of linear expansion of 4.47×10^{-6} 1/°C. In addition to Li *et al*, Talwar[7] *et al* also found a similar trend in the coefficient of thermal expansion plus the coefficient of linear expansion of 3.5×10^{-6} 1/°K.

5. SiC Volume Phase Grating

Here the 6H-SiC volume phase grating used in this manuscript is illustrated and no change occurred after being annealed up to 399°C. Shown below are optical microscope images of the SiC grating at 10X and 50X.

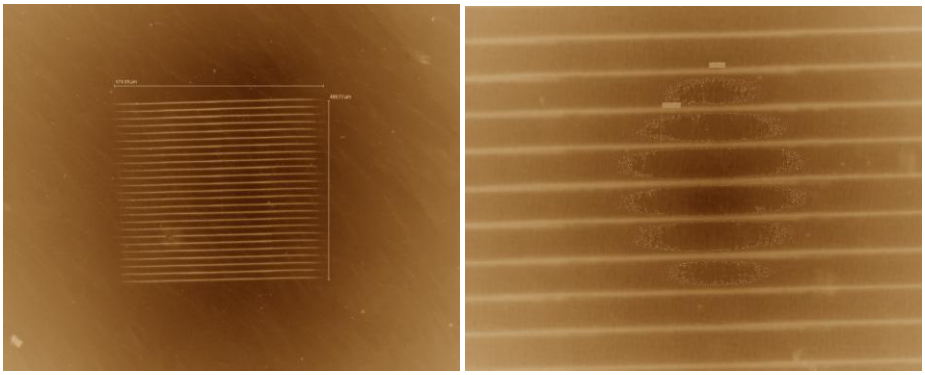

Figure 4 (Left) is the SiC grating at 10X magnification, and (Right) is the SiC grating after 50X magnification. The images were processed to view easier, and the images were obtained using Nomarski DIC on an optical microscope.

The 6H-SiC grating above was micro-machined using three anamorphic femtosecond laser lines in series with approximately 10µm of overlap between each anamorphic processed line. Each processed line has 3µm x 190µm dimensions and have a 20µm grating spacing. The overlap of the three lines causes a complex diffraction pattern described using Fourier analysis[8] of this grating convoluted with a Gaussian HeNe beam. The mathematical transmittance function of this grating convoluted with the HeNe beam is shown in Equation 7 below.

$$t_a(x,y)=\left[\left\{e^{-\pi\left(\frac{x^2}{A^2}+\frac{y^2}{B^2}\right)}+e^{-\pi\left(\frac{(x\pm x_0)^2}{A^2}+\frac{y^2}{B^2}\right)}\right\}\otimes\left\{\left[\frac{1}{L}\cdot comb\left(\frac{y}{L}\right)\cdot\delta(x)\right]\cdot rect\left(\frac{y}{NL}\right)\right\}\right]\bullet e^{-\pi\cdot\frac{r^2}{{\omega_o}^2}}\right] \quad \text{Equation 7}$$

The first two terms in Equation 7 represent the femtosecond micro-machined processed anamorphic lines (3 lines), which is convoluted with the grating comb function and multiplied by the HeNe Gaussian function for spot size, ω_o. The variables A and B represent the width and length of the processed grating lines, and L is the grating spacing. The femtosecond beam is also represented using a Gaussian function for simplicity, but is actually a secant-squared function. Below gives the theoretical and experimental results of the diffraction pattern as stated above.

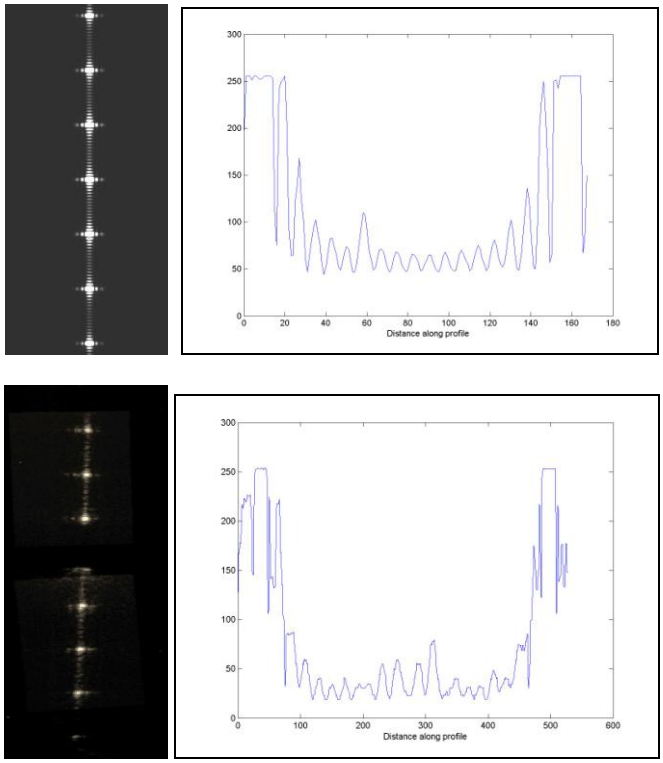

Figure 5 (Above) is the theoretical Fraunhofer diffraction pattern with a lineout of two of the orders, (Below) is the experimental Fraunhofer diffraction pattern with a lineout of two of the orders.

Figure 5 above shows very good agreement with theory and experimental results. Order spacing and number of minor orders agree, however, the 1st and 2nd order peaks saturate the CCD camera so it is uncertain if their amplitudes agree, but considering they both saturate and the minor orders agree it can be assumed that they are in close agreement considering the method of which the data was acquired with a common digital camera. The experimental results were collected using a common digital camera and a lineout performed using Matlab code. From the model the grating structure can be designed to provide the desired diffraction pattern if needed. These results show primarily that the SiC grating structure morphology is understood since the optical microscope may not illustrate or provide enough evidence as to what the structure is exactly.

6. Conclusion

In this work we report a new noncontact method of measuring the thermal coefficient of transparent and nontransparent materials using diffraction gratings. This paper also reports the measurement of 6H-SiC coefficient of the nonlinear thermal expansion and coefficient of linear expansion. Finally, a new high temperature sensor using gratings micro-machined in 6H-SiC was developed that can be used for high temperatures.

The temperature sensor deflection results can also be improved by adding a lens one focal length away from the stop of the system to create a telescentric or parallel focused beams at the focus plane that representing each order. The lens will then provide an order of magnitude higher resolution, which will increase temperature measurement sensitivity. Special thanks are given to AFRL personal at WPAFB, the University of Dayton, and Dr. Frank Baxely for assisting in discussions regarding these measurements.

7. References

[1] L. DesAutels, C. Brewer, M. Walker, S. Juhl, M. Finet, P. Powers, "Femtosecond micromachining in transparent bulk materials using an anamorphic lens," Optics Express, **15**, 20, 13139-13148 (2007).

[2] J. Copper, Purdue Wide Band Gap Semiconductor Device Research Program, http://www.ecn.purdue.edu/WBG/Index.html, Purdue University College of Engineering.

[3] R. Serway, "Physics For Scientists & Engineers," 3rd edition, 513-515, (1999).

[4] C. Palmer, "Diffraction Grating Handbook," Richardson Grating Laboratory (2002).

[5] R.T. Bhatt, A.R. Palczer, "Effects of Thermal Cycling on Thermal Expansion and Mechanical Properties of SiC Fiber-Reinforced Reaction-Bonded Si3N4 Composites," NASA Technical Memorandum 106665/Army Research Laboratory, 1-15, (1992).

[6] Z. Li, R. Bradt, "Thermal Expansion of the Hexagonal (4H) Polytype of SiC," J. Appl. Phys., **60**, 2, 612-614, (1986).

[7] D.N. Talwar, J.C. Sherbondy, "Thermal expansion coefficient of 3C-SiC," Appl. Phys. Lett. **67**, 22, 3301-3303, (1995).

[8] J.W. Goodman, "Introduction to Fourier Optics," Roberts and Company, ISBN 0-9747077-2-4, (2005).